Inorganic Chemistry

Article

pubs.acs.org/IC

Coordination Networks of a Ditopic Macrocycle Exhibiting Anion-Controlled Dimensional Changes and Crystal-to-Crystal Anion Exchange

Eunji Lee,[†] Ki-Min Park,[†] Mari Ikeda,[‡,§] Shunsuke Kuwahara,[§,∥] Yoichi Habata,*[,§,∥] and Shim Sung Lee*[,†]

[†]Department of Chemistry and Research Institute of Natural Science, Gyeongsang National University, Jinju 660-701, South Korea

[‡]Education Center, Faculty of Engineering, Chiba Institute of Technology, 2-1-1 Shibazono, Narashino, Chiba 275-0023, Japan

[§]Research Center for Materials with Integrated Properties and [∥]Department of Chemistry, Faculty of Science, Toho University, 2-2-1Miyama, Funabashi, Chiba 274-8510, Japan

Supporting Information

ABSTRACT: A rationally designed NO_2S_2-donor macrocycle **L** was synthesized, and anion variation (PF_6^-, $CF_3CO_2^-$, NO_3^-, and $CF_3SO_3^-$) of its silver(I) complexes was employed as a strategy for controlling their coordination modes and network dimensions. The assembly reactions of **L** with four silver(I) salts afforded the complexes $[Ag_2L_2](PF_6)_2$ (**1**), $[Ag_4L_2(CF_3CO_2)_4]_n$ (**2**), $[Ag_4L_2(NO_3)_4]_n$ (**3**), and $\{[Ag_3L_2(CF_3SO_3)_2]CF_3SO_3\}_n$ (**4**) that adopt cyclic dimer, 1D, 2D, and pseudo 3D network structures, respectively, with the structure adopted depending on the coordination ability and coordination modes of the anion used. Interestingly, quantitative anion exchange accompanying an irreversible structural conversion from **2**, **3**, or **4** to **1** was observed in the crystalline state by powder X-ray diffraction (PXRD) and IR spectroscopy. A stepwise mechanistic process from **2** ($CF_3CO_2^-$, 1D) to **3** (NO_3^-, 2D) by anion exchange was also proposed.

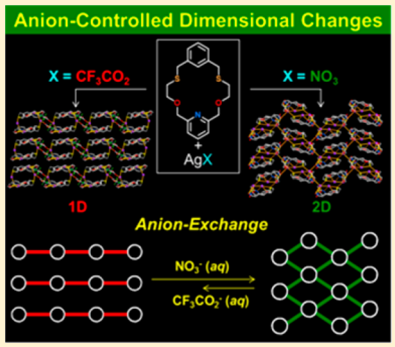

INTRODUCTION

The rational design of host ligand systems for the programmed self-assembly of metallosupramolecules via coordinative networking has attracted intense interest not only because of the fascinating structures generated but also because of their potential applications.[1] This is also true for macrocyclic host systems, which bind the metal ion inside the cavity (endocoordination).[2] However, the networking of macrocycles upon complexation brought by the endocoordination mode has severe limits due to tying up the metal center in the cavity by the bound macrocycle. Thus, very often the use of bridging organic coligands or coordinating anions leads to the networking of individual macrocyclic complex units to give larger oligomer or polymer structures.[3] In the case of bound anions, these can also act as potential (anion) exchange sites for the construction of new supramolecular entities.[4]

Exocyclic coordination (or exocoordination), in which the metal binds outside the macrocyclic cavity, has been employed as an alternate means for inducing the networking of macrocyclic species.[5] In particular, sulfur-containing thiamacrocycles often exhibit metal exocoordination due to inherent electronic and steric influences associated with the presence of the sulfur donors.[6] However, exocoordination-based networking of metal-bound macrocycles as a means of directing the formation of assembled products displaying zero to higher dimensional topologies had remained largely unexplored, even though a range of exocyclic macrocyclic complex products have been reported.[7]

We have been involved in a series of investigations aimed at preparing new types of exo- and endo/exocoordinated macrocyclic complexes. In this regard, several examples of silver(I) complexes showing anion-controlled endo- or exocoordination,[8] heterometallic endo/exocoordinated networks,[9] solvent-induced single-crystal-to-single-crystal transformation of endo/exocyclic silver(I) coordination polymers,[10] cation-selective/anion-controlled chromogenic mercury(II) sensors in solution,[11] and solid[12] states have all been demonstrated.[8−12] Indeed, the silver(I) ion with its d^{10} electron configuration (being free of crystal field effects) readily binds to macrocyclic ligands with S, S/O, and N/O donors to form products with a variety of coordination arrangements that commonly include endo- and/or exocyclic coordination modes.[7a,13]

In the course of our ongoing studies to prepare new types of macrocyclic network complexes containing simultaneous endo- and exocoordination, we have been interested in merging individual controlling factors elucidated previously for the design of new macrocyclic ligand systems.[5] For example, a primary task here was to investigate the dual coordination mode of the proposed NO_2S_2-macrocycle **L** that was anticipated to bind metal ion(s) in defined position(s) inside and/or outside of the cavity (Schemes 1 and 2). In particular, the introduction of one pyridine unit into the macrocyclic

Received: February 20, 2015
Published: May 8, 2015

DOI: 10.1021/acs.inorgchem.5b00422
Inorg. Chem. 2015, 54, 5372−5383

Scheme 1. Influence of the Ligand and Anion on the Coordination Mode and Networking

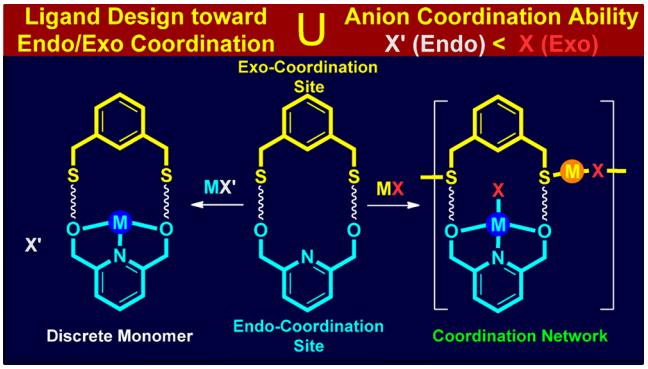

Scheme 2. Synthesis of L

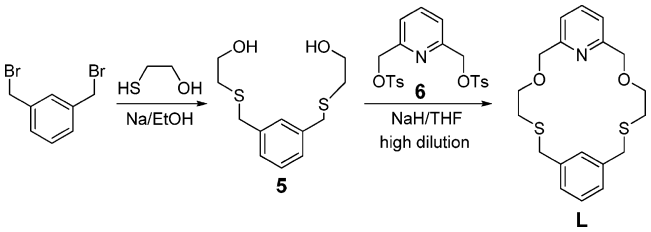

donor set coupled with the expected exocoordination of the sulfur donors could induce the formation of desired endo/exocoordinated network species. In addition to generating discrete or polymeric structures based on endo/exocoordination, control of the dimensionality of the polymeric systems was another goal of interest. Thus, in the present work, the use of several anions with different coordinating abilities and bridging modes was employed. This strategy was expected to prepare distinct endo- and/or exocoordinated complexes of **L** with discrete or polymeric structures with the coordination modes being as depicted in Scheme 1, with the overall crystal topologies having different dimensionalities that are anion dependent.

In this study, we prepared four silver(I) complexes of **L**, displaying different coordination modes (endo/endo and endo/exo) and topologies (dimer and network) that clearly depend on the nature of the anions (PF_6^-, $CF_3CO_2^-$, NO_3^-, and $CF_3SO_3^-$) used. Changing $CF_3CO_2^-$ to NO_3^- or $CF_3SO_3^-$ resulted in dimensional changes of the resulting solid-state network structures from 1D to 2D or pseudo 3D. These anion-controlled structural differences in the crystalline state have been systemically investigated, and a stepwise mechanistic process for the unique structural transformations accompanying the dimensional changes has been proposed.

RESULTS AND DISCUSSION

Ligand Design and Synthesis. The macrocycle **L** has lower symmetry arising from the introduction of both endo- and exocoordination domains (Scheme 1). In an attempt to induce endocyclic coordination, one pyridine and two ether oxygen donors were introduced. The relatively large separation of the two sulfur donors in the 1,3-benzylic positions is expected to result in each sulfur donor coordinating to individual metal ions, with the presence of both endo- and exocoordination sites expected to result in endo/exocoordinated complexes.[5a,14]

The bimolecular ditosylate−diol macrocyclization reaction enables the preparation of macrocycles via C−O bond formation, with macrocycle **L** being synthesized by coupling reactions between diol **5** and ditosylate **6** in the presence of sodium hydride under high dilution conditions (yield, 30%; Scheme 2). Compounds **5** and **6** were prepared using known literature procedures.[15] The NMR spectra of **L** exhibit some signal complexity due to its unsymmetrical nature (Figures S1 and S2, Supporting Information) but is in accord with the target structure.

Crystal Structure of L. The structure of **L** is shown in Figure 1. Single crystals of **L** were grown by slow evaporation

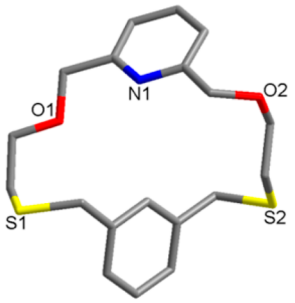

Figure 1. Crystal structure of **L**. Torsion angles between selected adjacent donors are S1−C−C−O1 (72.1°), O1−C−C−N1 (42.3°), N1−C−C−O2 (150.0°), and O2−C−C−S2 (173.6°).

from its dichloromethane solution. In the structure, the pyridine nitrogen and one oxygen (O2) are directed toward the cavity center while both sulfur atoms and oxygen (O1) are oriented in an exo fashion. Accordingly, the S1···S2 distance (7.60 Å) in **L** is larger than that for O1···O2 (6.10 Å). From the torsion angles in the ligand backbone associated with the orientation of the donors, the conformation of the S1−O1−N1−O2−S2 linkage in the macrocycle unit can be described as *g-g-t-t* (*t* = trans, *g* = gauche).

Synthesis and Structural Description of the Silver Complexes Incorporating Different Anions. The influence of changing the anion on the coordination modes and network dimensions of the silver(I) complexes of **L** was investigated. As mentioned already, the use of four silver(I) salts resulted in the formation of discrete to pseudo 3D polymeric products when the syntheses were performed under related conditions (Scheme 3).

Reaction of **L** with $AgPF_6$ in dichloromethane/methanol yielded colorless crystals suitable for X-ray analysis. The crystal structure showed the product to be an unusual dinuclear bis(macrocycle) species of type $\{[Ag_2L_2](PF_6)_2$ (**1**) in which no anion or solvent molecules are present in its coordination sphere (Figure 2 and Table 1). Selected structural parameters are listed in Table 2. Due to the inversion symmetry, the asymmetric unit contains one **L** molecule, one Ag atom, and one PF_6^-. In **1**, the endocyclic Ag1 atom which lies inside the cavity is five coordinate, being bound to the NO_2S donors from one **L**. Notably, the remaining one site is occupied by one S donor (S2A) from an adjacent **L** to form a dimeric arrangement.

The silver(I) center in **1** can be considered as being in a distorted square pyramidal environment (τ value = 0.125).[16] The bridging Ag1−S2A [2.452(1) Å] bond is shorter than Ag1−S1 [2.568(1) Å] in the same plane, but both are within the normal range for this bond type. The Ag1−O1 bond

DOI: 10.1021/acs.inorgchem.5b00422
Inorg. Chem. 2015, 54, 5372−5383

Scheme 3. Silver(I) Complexes Prepared in This Work

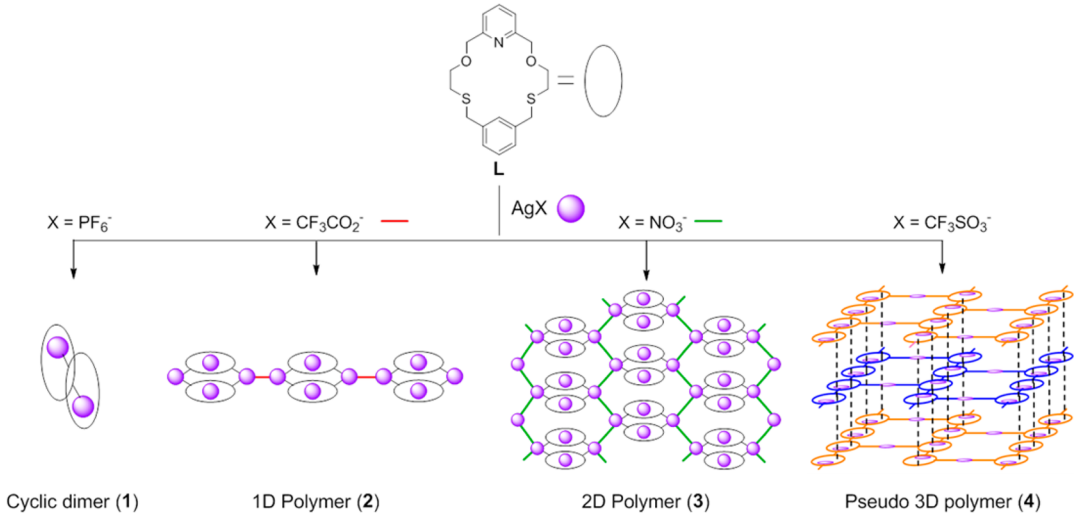

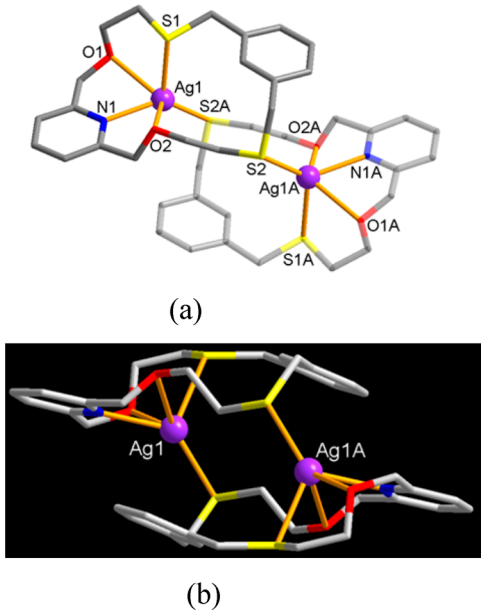

Figure 2. (a) Discrete cyclic dimer structure of the silver(I) hexafluorophosphate complex **1**, $[Ag_2L_2](PF_6)_2$. (b) Side view showing its dinuclear sandwich-type structure. Noncoordinating anions are omitted.

distance [2.638(2) Å] is typical, but that of the Ag1−O2 bond [3.038(3) Å] lies at the longer end of the database range [2.40−3.06 Å].[17]

In terms of the conformational changes of the ligand upon complexation, O2 and S1 donors in **1** are oriented toward the inside of the macrocyclic cavity. Accordingly, the S1···S2 distance (5.86 Å) in **1** is shorter than in free **L** (7.60 Å) but still large enough to induce the two sulfur donors to bind to two different metal ions.[14a] Hence, the metal center in **1** is shielded by the bound macrocycles from the anion and solvent molecules. The formation of this structure is also likely influenced by the weaker coordinating ability of the PF_6^- anion.[18] Consequently, the preferred anion/solvent noncoordinated cyclic dimer structure obtained presumably reflects that when the coordination ability of the anion is weak two adjacent complex units interact directly to form a discrete dimer. With respect to this, cyclic oligomeric complexes of macrocycles (including cyclic dimers) have been recently reviewed by us.[5b]

As outlined in Scheme 1, we examined the ditopic behavior of **L** by employing different silver(I) salts. When silver(I) trifluoroacetate was used under the same reaction conditions to those employed for silver(I) hexafluorophosphate, a colorless crystalline product **2** suitable for X-ray analysis was isolated. Unlike the discrete structure of **1**, the crystal structure showed that **2** is a 1D polymeric complex of type $[Ag_4L_2(CF_3CO_2)_4]_n$, in which two crystallographically independent silver atoms (Ag1 and Ag2) are positioned inside (Ag1) and outside (Ag2) the cavity (Figure 3). Selected structural parameters are given in Table 3. In this case, two endocyclic silver(I) complex units are bridged by two exocyclic silver(I) centers to generate a tetranuclear bis(macrocycle) unit which is further linked by two bidentate trifluoroacetate ions to give a 1D polymer structure. The asymmetric unit contains one **L**, two Ag atoms, and two trifluoroacetate ions. In **2**, the endocyclic Ag1 atom is five coordinate, being bound to NO_2S donors from one **L**, with the fifth site occupied by one monodentate trifluoroacetate ion. The exocyclic Ag2 atom is four coordinate, being bound to two sulfur donors (S1 and S2A) from two adjacent **L** ligands, with the remaining two sites occupied by two monodentate bridging trifluoroacetate ions. In connecting the tetranuclear bis(macrocycle) units, the two bridging trifluoroacetate ions and two silver atoms form an octagonal cycle, and this metallacyclization limits the topology of the resulting product to be one dimensional.[19] The separation of the two aromatic rings (centroid-to-centroid distance 5.54 Å) in the adjacent macrocycles is well outside the range expected for a $\pi-\pi$ stacking interaction.[20] The S1···S2 distance (6.27 Å) in **2** is shorter than that in free **L** (7.60 Å) but longer than that (5.86 Å) in **1**, which allows the two sulfur donors to bind two different endocyclic silver atoms. Compared with the noncoordinating nature of PF_6^- in **1**, the influence of the coordinating ability of $CF_3CO_2^-$ in **2** to induce the endo/exocoordination as well as the linking the bis(macrocycle) complex units to form a 1D polymer chain is noteworthy.

The preparation of the anion-dependent silver(I) complexes **1** and **2** displaying different dimensions encouraged us to probe the possible formation of corresponding coordination networks with higher dimensions. We assumed that the use of smaller

DOI: 10.1021/acs.inorgchem.5b00422
Inorg. Chem. 2015, 54, 5372−5383

Table 1. Crystal and Experimental Data

	L	1	2	3	4
formula	$C_{19}H_{23}N_1O_2S_2$	$C_{19}H_{23}Ag_2P_1F_6N_1O_2S_2$	$C_{23}H_{23}Ag_2F_6N_1O_6S_2$	$C_{19}H_{23}Ag_2N_3O_8S_2$	$C_{20.5}H_{23}Ag_{1.5}F_{4.5}N_1O_{6.5}S_{3.5}$
fw	361.50	614.34	803.28	701.26	746.91
temp (K)	173(2)	173(2)	173(2)	173(2)	173(2)
cryst syst	triclinic	monoclinic	triclinic	monoclinic	orthorhombic
space group	*P*-1	$P2_1/n$	*P*-1	$P2_1/c$	*Pccn*
Z	2	4	2	4	8
a (Å)	9.3283(2)	11.2267(2)	9.51350(10)	15.0491(8)	10.1091(3)
b (Å)	10.2295(2)	17.0130(3)	11.5738(2)	18.8422(10)	19.8081(6)
c (Å)	10.6795(2)	12.2564(2)	13.9234(2)	8.0315(4)	25.7293(7)
α (deg)	87.9530(10)	90	107.5140(10)	90	90
β (deg)	71.8170(10)	108.1490(10)	101.7770(10)	91.875(2)	90
γ (deg)	67.7530(10)	90	97.0910(10)	90	90
V (Å^3)	892.17(3)	2224.51(7)	1402.88(3)	2276.2(2	5152.1(3)
D_{calcd} (g/cm^3)	1.346	1.834	1.902	2.046	1.926
$2\theta_{max}$ (deg)	52.00	56.00	56.00	56.00	56.00
R_1, wR_2 [$I > 2\sigma(I)$]	0.0300, 0.0777	0.0383, 0.0929	0.0218, 0.0470	0.0656, 0.1855	0.0248, 0.0558
R_1, wR_2 [all data]	0.0341, 0.0814	0.0453, 0.0980	0.0285, 0.0499	0.0708, 0.1884	0.0318, 0.0598
goodness-of-fit on F^2	1.032	1.005	1.017	1.050	1.011
no. of reflns used [$>2\sigma(I)$]	3477 [R_{int} = 0.0226]	5365 [R_{int} = 0.0306]	6750 [R_{int} = 0.0238]	5497 [R_{int} = 0.0337]	6225 [R_{int} = 0.0463]
refinement	full matrix	full matrix	full matrix	full matrix	full matrix

Table 2. Selected Bond Lengths (Angstroms) and Bond Angles (degrees) for 1, $[Ag_2L_2](PF_6)_2$[a]

Ag1−N1	2.299(2)	Ag1−O1	2.638(2)
Ag1−O2	3.038(3)	Ag1−S1	2.568(1)
Ag1−S2A	2.452(1)		
N1−Ag1−S1	102.8(1)	N1−Ag1−O1	69.2(1)
N1−Ag1−O2	64.2(1)	N1−Ag1−S2A	133.0(1)
O1−Ag1−O2	119.4(1)	S1−Ag1−O1	74.6(1)
S1−Ag1−O2	80.2(1)	O1−Ag1−S2A	114.3(1)
O2−Ag1−S2A	125.5(1)	S1−Ag1−S2A	123.7(1)

[a]Symmetry operations: (A) $-x + 1, y, -z + 1$.

multidentate anions with trigonal or tetrahedral shapes might lead to the formation of not only endo/exocoordination but also higher dimensional networks.[7a,21] In fact, the role of the anions on the dimensionality of silver(I) adducts for the linear ligand system has been largely investigated.[22]

When silver(I) nitrate was used in the reaction with **L**, crystalline product **3** was isolated. Compound **3** features a 2D polymeric structure of type $[Ag_4L_2(NO_3)_4]_n$ in which two crystallographically different silver(I) ions are positioned inside (Ag1) and outside (Ag2) the cavity (Figure 4). Again, bridging of two endocyclic silver(I) complex units by two exocyclic silver(I) atoms affords a tetranuclear bis(macrocycle) unit which is further linked by one nitrate ion to give a 1D polymeric wavy chain. The parallel 1D wavy chains are cross-linked by another bridging nitrate ion to generate a 2D network structure (Figure 4a−c). The asymmetric unit in **3** contains one **L** molecule, two Ag atoms, and two nitrate ions.

The Ag1 atom in the macrocyclic cavity is five coordinate, being bound to NO_2S donors (N1, O1, O2, and S1) from one **L**, with the fifth site occupied by one monodentate terminal nitrate ion (Figure 4d and Table 4). The Ag2 atom outside the cavity is four coordinate, being bound to two sulfur donors (S1 and S2A) from two adjacent **L** ligands with the two sites occupied by two monodentate bridging nitrate ions. Additionally, face-to-face $\pi-\pi$ stacking interactions between two adjacent macrocycles is observed (dashed line in Figure 4d), with the centroid-to-centroid distance between the two aromatic rings involved being 4.56 Å; this falls at the long end of the literature range (3.7−4.6 Å) for such an interaction.[20]

As an extension of the above, when silver(I) trifluoromethanesulfonate was employed a pseudo 3D polymeric product of type $\{[Ag_3L_2(CF_3SO_3)_2]CF_3SO_3\}_n$ (**4**) was isolated (Figure 5). The asymmetric unit of **4** contains 1 **L** molecule, 1.5 Ag atoms, 1 coordinated $CF_3SO_3^-$, and 0.5 uncoordinated $CF_3SO_3^-$. Again, there are two kinds of Ag atoms (Ag1 and Ag2) occupying different positions and showing different coordination environments. Thus, the Ag1 atom inside the cavity is five-coordinate, being bound to NO_2S donors from one **L**, with the remaining site occupied by one S donor (S2A) from an adjacent **L** to form a 1D polymeric chain via Ag1−S2A bond [2.476(1) Å] formation, Table 5. The adjacent 1D chains are cross-linked by Ag2 atoms outside the cavity via an Ag2−S1 bond [2.552(1) Å], resulting in the formation of a brick-wall-type 2D polymer structure. One brick unit consists of eight Ag atoms and six macrocycles (Figure 5c). The exocyclic Ag2 atom is four coordinate, and its coordination sphere is completed by two $CF_3SO_3^-$ ions as terminal monodentate ligands, with a Ag2−O3 bond distance of 2.415(2) Å. As a result, the anion in **4** does not participate in the networking of the resulting structure. This contrasts with the situation in **2** and **3** in which the anions link the metal centers as linker ligands and lead to the formation of the observed higher dimensional topologies. The preferred infinite endo/exocyclic 2D structure of **4** is also associated with the role of one sulfur donor (S1) which coordinates to the endocyclic Ag1 and exocyclic Ag2 atoms simultaneously.

In the packing structure of **4**, the face-to-face $\pi-\pi$ stacking interaction (centroid-to-centroid distance 3.61 Å) between two layers allows the formation of the pseudo 3D polymeric structure (dashed lines in Figure 5a). The surrounding empty space is occupied by disordered $CF_3SO_3^-$ ions stabilized by CH···F H bonding (Figure S4, Supporting Information). This is a rare case in which a high-dimensional structure of a

DOI: 10.1021/acs.inorgchem.5b00422
Inorg. Chem. 2015, 54, 5372−5383

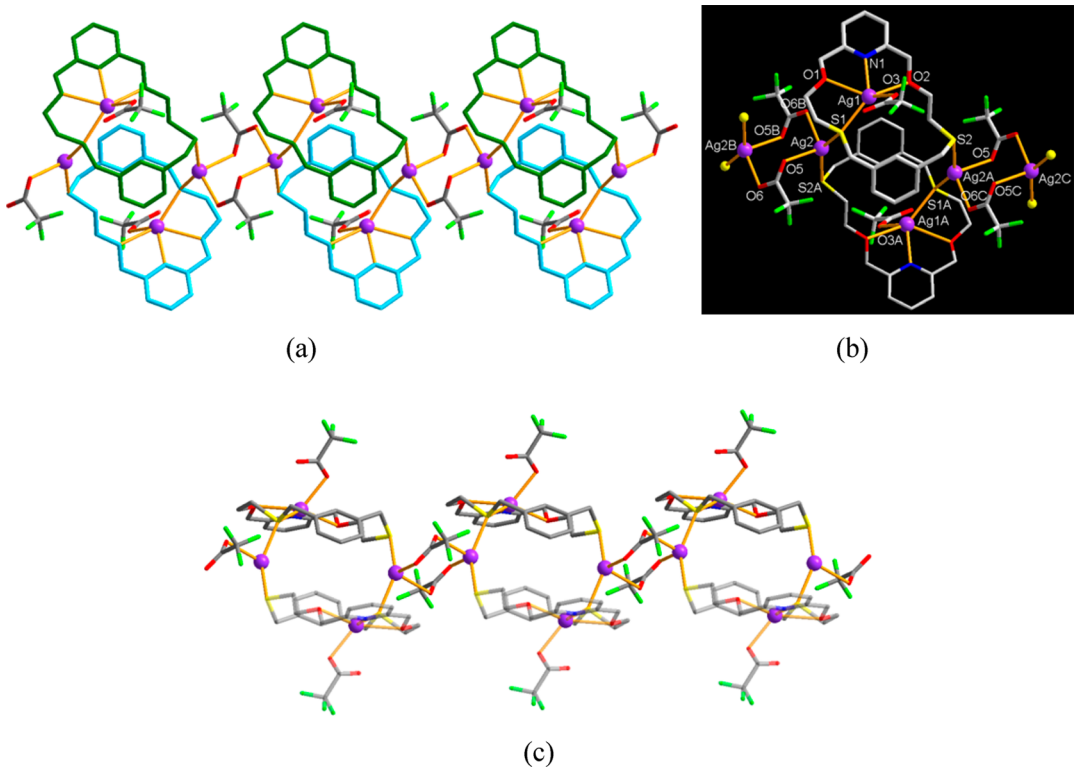

Figure 3. (a) 1D polymeric structure of the silver(I) trifluoroacetate complex **2**, $[Ag_4L_2(CF_3CO_2)_4]_n$. (b) View of the coordination environments. (c) Side view.

Table 3. Selected Bond Lengths (Angstroms) and Bond Angles (degrees) for 2, $[Ag_4L_2(CF_3CO_2)_4]_n$[a]

Ag1−N1	2.315(2)	Ag1−O1	2.615(1)
Ag1−O2	2.594(1)	Ag1−O3	2.337(2)
Ag1−S1	2.491(1)	Ag2−O5	2.549(1)
Ag2−O6B	2.370(1)	Ag2−S1	2.478(1)
Ag2−S2A	2.468(1)		
N1−Ag1−O1	65.5(1)	N1−Ag1−O2	68.8(1)
N1−Ag1−O3	107.0(1)	N1−Ag1−S1	130.2(1)
O1−Ag1−O2	133.4(1)	O1−Ag1−O3	123.8(1)
O1−Ag1−S1	73.4(1)	O2−Ag1−O3	78.1(1)
O2−Ag1−S1	136.2(1)	O3−Ag1−S1	119.0(1)
O5−Ag2−O6B	99.8(1)	O5−Ag2−S1	90.4(1)
O5−Ag2−S2A	100.3(1)	O6B−Ag2−S1	100.5(1)
O6B−Ag2−S2A	110.3(1)	S1−Ag2−S2A	144.8(2)

[a]Symmetry operations: (A) $-x + 2, -y + 1, -z + 1$. (B) $-x + 2, -y + 2, -z + 1$.

macrocyclic ligand system is formed without direct anion involvement.

Photophysical Properties. The photoluminescence properties of **L** and its silver(I) complexes **1**−**4** were investigated in the solid state (Figure 6). While free **L** shows no significant emission, its complexes display blue photoluminescence resulting from the $\pi-\pi^*$ transition in the respective aromatic moieties. For each complex the emission intensity of the complexes may likely be enhanced through the presence of the endo/exocyclic metal coordination by the macrocyclic ligand which increases the structural rigidity of the ligand and thereby reduces the loss of energy by nonradiative decay.[23] The emission spectra of **1**, **2**, **3**, and **4** show maxima at 428, 409, 410, and 419 nm, respectively. Among the polymeric species, **4** shows a red-shifted peak (419 nm) with the highest intensity, perhaps reflecting the presence of the interlayer $\pi-\pi$ stacking interactions between aromatic units in the solid state as seen in its X-ray structure (Figure 5a).

Thermal Stability. TGA analyses were performed in order to investigate the thermal stabilities of **1**−**4** (Figure 7). The TGA curves revealed that the thermal stabilities of **1**−**4** are not very different. For example, the PF_6^--containing dimer **1** is stable up to 222 °C, while the TGA curves for the polymeric products **2**, **3**, and **4** indicate no loss of solvent molecules occurs until 210, 200, and 240 °C, respectively, in accord with the presence of tightly packed solid-state structures. This result is also consistent with the high calculated densities of **2**, **3**, and **4** (D_{calcd} = 1.834−2.046) found for these structures (Table 1). Further heating of each complex up to ∼450 °C resulted in complex decomposition.

Structural Transformation via Anion Exchange in the Crystalline State. Since the anion-dependent products **1**−**4** with different dimensionalities are insoluble in water and common organic solvents, structural conversion of these products by anion exchange in the crystalline state was investigated. Each crystalline sample was immersed in a 3 M aqueous solution of the sodium salt of the required anion, and the solid was periodically collected by filtration. The structural conversions associated with anion exchange in the respective solids were systemically monitored by their PXRD patterns and IR spectra.

Interestingly, in particular cases the anion-exchange procedure induced a dimensional increase in the crystalline sample. For example, when **2** was immersed in 3 M $NaNO_3$ aqueous solution and left undisturbed at ambient temperature to allow anion exchange, the PXRD patterns for the samples collected after 0.5 and 1 h show a decreased intensity for **2** (red square in Figure 8a) and an increased intensity for **3** (green

DOI: 10.1021/acs.inorgchem.5b00422
Inorg. Chem. 2015, 54, 5372−5383

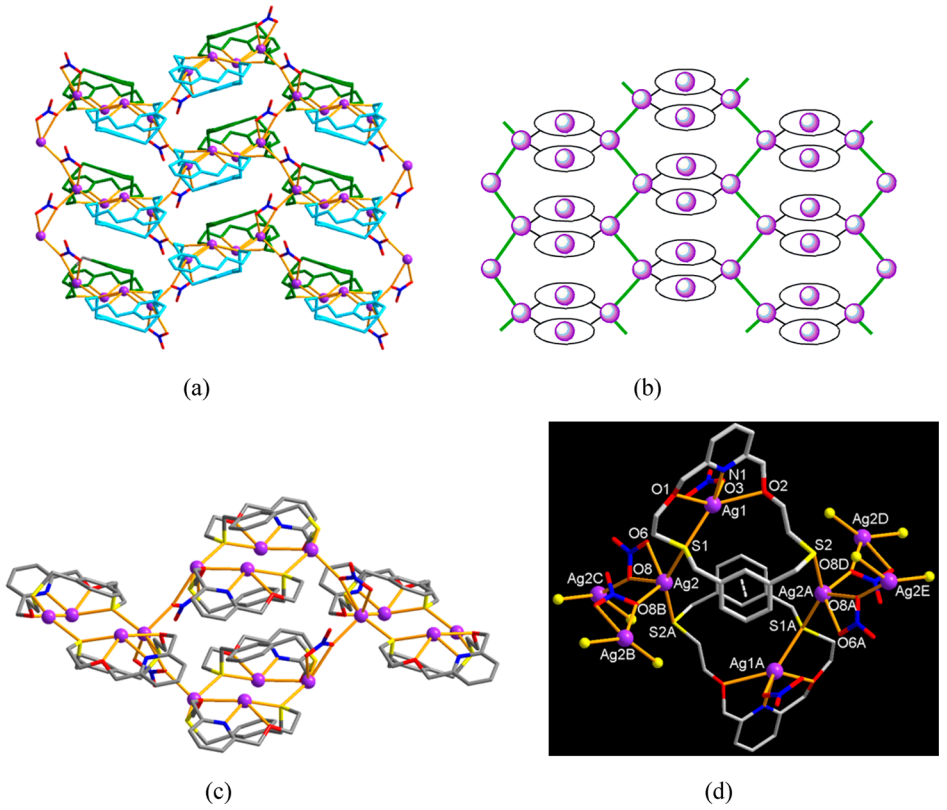

Figure 4. (a) 2D polymeric network structure of silver(I) nitrate complex **3**, $[Ag_4L_2(NO_3)_4]_n$, showing two types of anion linking. (b) Schematic presentation of the 2D network. (c) One block unit with four tetranuclear bis(macrocycle) subunits. (d) View of the coordination environments.

Table 4. Selected Bond Lengths (Angstroms) and Bond Angles (degrees) for 3, $[Ag_4L_2(NO_3)_4]_n$[a]

Ag1–N1	2.324(7)	Ag1–O1	2.597(6)
Ag1–O2	2.630(6)	Ag1–O3	2.412(2)
Ag1–S1	2.551(2)	Ag2–O6	2.541(7)
Ag2–O8B	2.445(7)	Ag2–S1	2.553(2)
Ag2–S2A	2.510(2)		
N1–Ag1–O1	66.7(2)	N1–Ag1–O2	68.8(2)
N1–Ag1–O3	97.7(6)	N1–Ag1–S1	133.0(2)
O1–Ag1–O2	134.3(2)	O1–Ag1–O3	127.7(8)
O1–Ag1–S1	73.4(2)	O2–Ag1–S1	136.8(1)
O2–Ag1–O3	68.2(5)	O3–Ag1–S1	126.6(4)
O6–Ag2–S1	86.4(2)	O6–Ag2–O8B	121.0(2)
O6–Ag2–S2A	111.8(2)	O8B–Ag2–S1	95.0(2)
O8B–Ag2–S2A	99.6(2)	S1–Ag2–S2A	145.4(1)

[a]Symmetry operations: (A) $-x + 1, -y + 1, -z + 1$. (B) $x, -y + 1.5, z - 0.5$.

circle in Figure 8a), indicating that partial anion exchange had occurred. Moreover, the PXRD pattern for the sample collected after 3 h was completely coincident with that of **3**, indicating that the 1D structure of **2** had been quantitatively converted to the 2D structure **3** by the exchange of $CF_3CO_2^-$ with NO_3^-.

The IR spectra are in accord with the above PXRD results. As shown in Figure 8b, the IR spectra for the samples collected after 0.5 and 1 h show the gradual disappearance of an intense $CF_3CO_2^-$ peak at 1685 cm^{-1} (red square) and the growth of a new NO_3^- band at 1383 cm^{-1} (green circle). The $CF_3CO_2^-$ peak disappears completely after 3 h, and the resulting IR spectrum does not differ significantly from that of **3**, suggesting that not only is the $CF_3CO_2^-$ ion quantitatively displaced by the NO_3^- ion but also the solid-state topology fully changes from 2D to 3D within 3 h.

To investigate the reversibility of the anion exchange between **2** and **3**, the insoluble crystals of **3** were immersed in 3 M $NaCF_3CO_2$ aqueous solution. As shown in Figure 9, the PXRD patterns and IR spectra for the samples collected after 2 days show decreased peak intensities for **3** (green circle) and the appearance of new peaks for **2** (red square), indicating the presence of a partially anion-exchanged sample. After 1 week under the same conditions, the peaks for **3** showed weaker intensities but were still present along with increased peak intensity for **2**, indicating that the anion exchange is not completely reversible, as only about 50% of NO_3^- could be exchanged with $CF_3CO_2^-$.

The above anion-exchange procedure can be extended to other anions. When **2**, **3**, and **4** were each immersed in a 3 M $NaPF_6$ aqueous solution and left undisturbed at ambient temperature, the PXRD pattern and IR spectrum for each sample collected after 12 h was completely coincident with that for **1**, indicating that **2**, **3**, and **4** (with polymeric structures) were each converted to the discrete dimer **1** quantitatively by the exchange of $CF_3CO_2^-$, NO_3^-, and $CF_3SO_3^-$ with PF_6^-, respectively (Figures S6–S8, Supporting Information). However, the PF_6^- in **1** did not exchange with $CF_3CO_2^-$, NO_3^-, and $CF_3SO_3^-$ even when **1** was immersed in the 3 M sodium salt solution with the chosen anion for 1 week. Similarly, $CF_3SO_3^-$ in **4** underwent complete exchange with $CF_3CO_2^-$ and NO_3^- to give **2** and **3**, respectively, when the crystals of **4** were immersed in an aqueous solution of $NaCF_3CO_2$ and $NaNO_3$ for 12 h (Figures S9 and S10, Supporting Information). However, the $CF_3CO_2^-$ in **2** and NO_3^- in **3** did not exchange with $CF_3SO_3^-$ under similar conditions.

DOI: 10.1021/acs.inorgchem.5b00422
Inorg. Chem. 2015, 54, 5372–5383

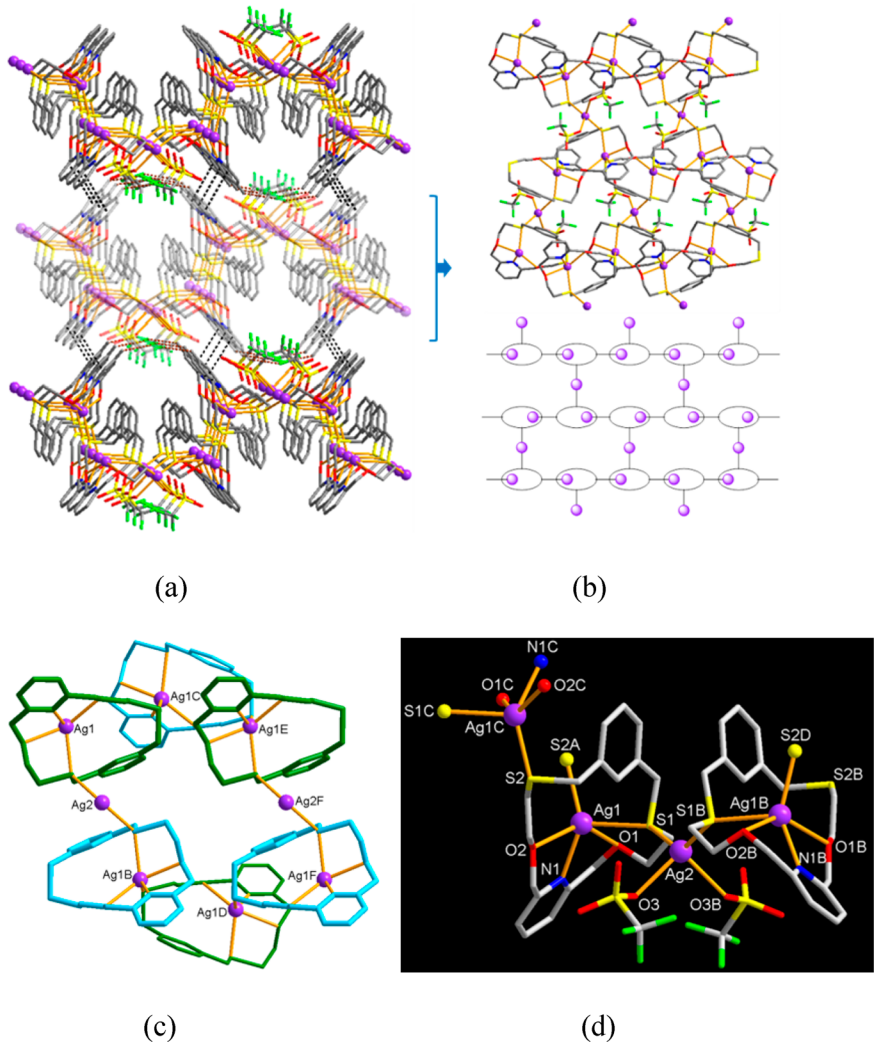

Figure 5. (a) Pseudo 3D polymeric structure of the silver(I) trifluoromethanesulfonate complex **4**, $\{[Ag_3L_2(CF_3SO_3)_2]CF_3SO_3\}_n$, formed via interlayer $\pi-\pi$ stacking (centroid-to-centroid distance 3.61 Å). (b) Brick-wall-type 2D layer structure. (c) One-brick unit (two terminal $CF_3SO_3^-$ ions coordinated to Ag2 atoms are omitted). (d) View of the coordination environments.

Table 5. Selected Bond Lengths (Angstroms) and Bond Angles (degrees) for 4, $\{[Ag_3L_2(CF_3SO_3)_2]CF_3SO_3\}_n$[a]

Ag1–N1	2.293(2)	Ag1–O1	2.603(2)
Ag1–O2	2.586(2)	Ag1–S1	2.655(1)
Ag1–S2A	2.476(1)	Ag2–O3	2.415(2)
Ag2–S1	2.552(1)		
N1–Ag1–O1	69.3(1)	N1–Ag1–O2	69.2(1)
N1–Ag1–S1	110.9(1)	N1–Ag1–S2A	140.0(1)
O1–Ag1–O2	138.3(1)	O1–Ag1–S1	74.5(1)
O1–Ag1–S2A	109.6(1)	O2–Ag1–S1	117.9(1)
O2–Ag1–S2A	104.3(1)	S2A–Ag1–S1	106.8(2)
O3–Ag2–O3B	90.8(1)	O3–Ag2–S1B	123.2(1)
O3–Ag2–S1	91.7(1)	S1–Ag2–S1B	131.5(1)

[a]Symmetry operations: (A) $x + 1/2, -y + 1, -z + 1/2$. (B) $-x + 1/2, -y + 3/2, z$.

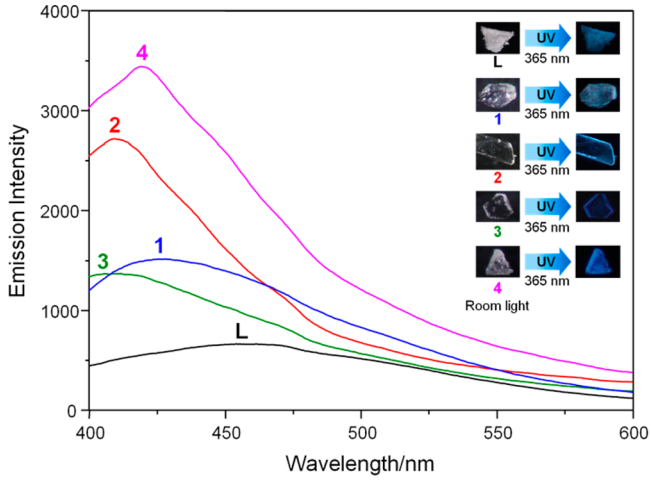

Figure 6. Solid-state photoluminescence spectra of **1**–**4** at room temperature (excitation at 360 nm).

The observed anion-exchange results are summarized in Scheme 4. All products displayed anion-exchange abilities, with PF_6^- being preferred over $CF_3CO_2^-$, NO_3^-, and $CF_3SO_3^-$. On the basis of the pairwise results, the anion exchanges show the following order: PF_6^- (**1**) > NO_3^- (**3**) > $CF_3CO_2^-$ (**2**) > $CF_3SO_3^-$ (**4**). The preference for PF_6^- and the lowest affinity for $CF_3SO_3^-$ follow the Hofmeister series,[24] which shows the order $PF_6^- \gg ClO_4^- > BF_4^- > CF_3CO_2^- > NO_3^- > Cl^- > CF_3SO_3^- > HCO_2^- > H_2PO_4^-$. However, the observed

DOI: 10.1021/acs.inorgchem.5b00422
Inorg. Chem. 2015, 54, 5372–5383

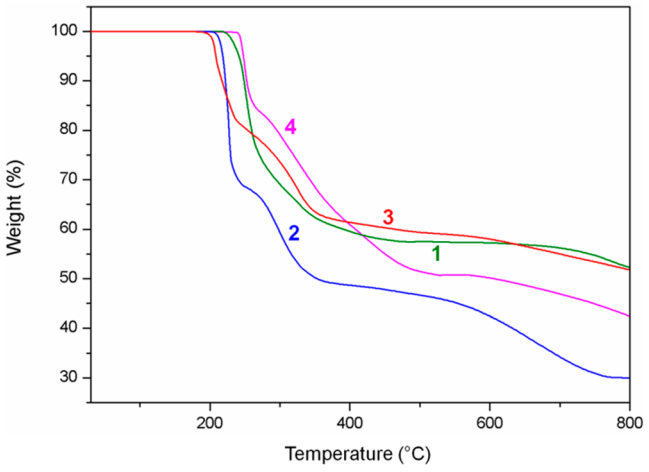

Figure 7. TGA curves for **1**–**4**.

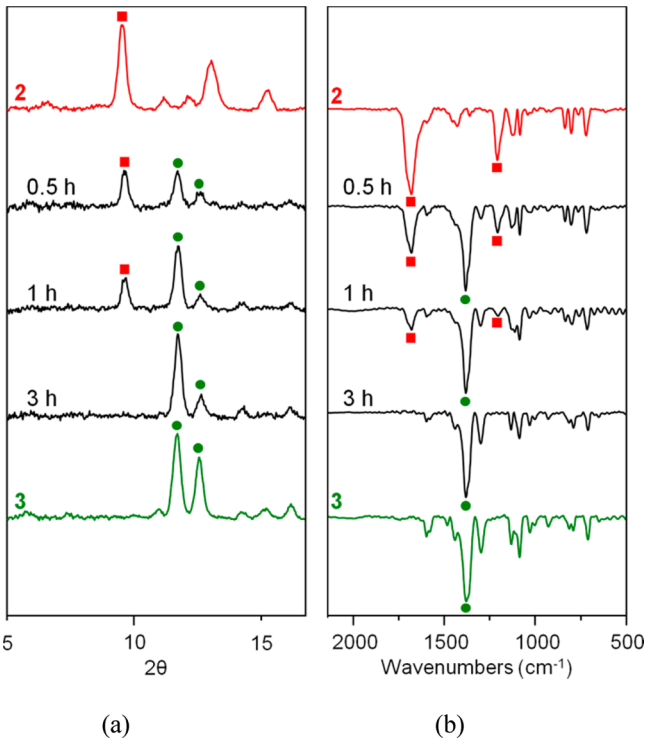

Figure 8. (a) PXRD patterns for **2** after anion exchange employing 3 M $NaNO_3$ aqueous solution for 0.5, 1, and 3 h. (b) IR spectra of **2** after anion- exchange employing 3 M $NaNO_3$ aqueous solution for 0.5, 1, and 3 h. Data shown in the top and bottom represent the PXRD patterns and the IR spectra for **2** and **3** prepared by direct synthesis, respectively.

preference of NO_3^- (**3**) over $CF_3CO_2^-$ (**2**) represents a deviation from the Hofmeister series. As already discussed, the anion exchange of $CF_3CO_2^-$ in **2** with NO_3^- to yield **3** is noteworthy because it occurs quantitatively in the crystalline state, accompanied by a dimensional increase from 1D to 2D.

There have been a few reports so far of structural transformations accompanying dimensional changes in the crystalline state when insoluble MOFs were treated with solvents.[25] These systems differ from the present ones in that the latter involve crystalline complexes and coordination polymers incorporating the ditopic macrocycle **L**, instead of the usual linear-ligand-based MOFs.[4,25] To the best of our

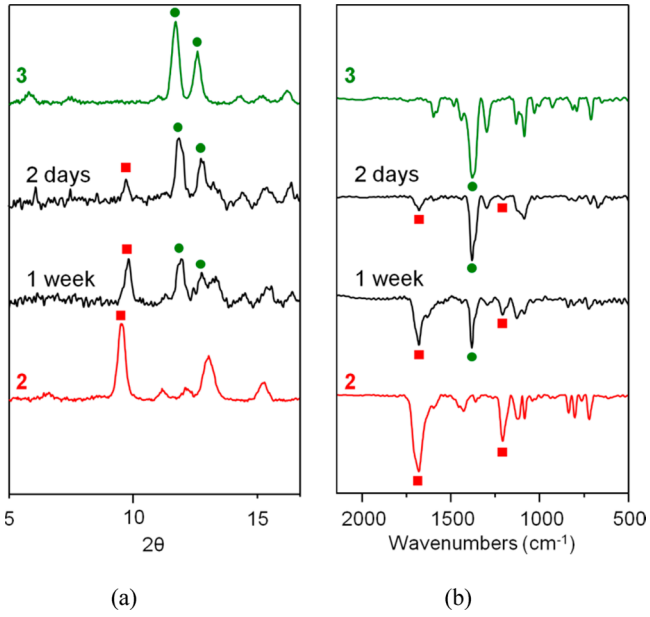

Figure 9. (a) PXRD patterns for **3** after anion exchange with 3 M $NaCF_3CO_2$ aqueous solution for 2 days and 1 week. (b) IR spectra for **3** after anion exchange with 3 M $NaCF_3CO_2$ aqueous solution for 2 days and 1 week. Data shown in the top and bottom represent the PXRD patterns and the IR spectra for **3** and **2** prepared by direct synthesis, respectively.

Scheme 4. Structural Transformation of 1–4 by Anion Exchange in the Crystalline State

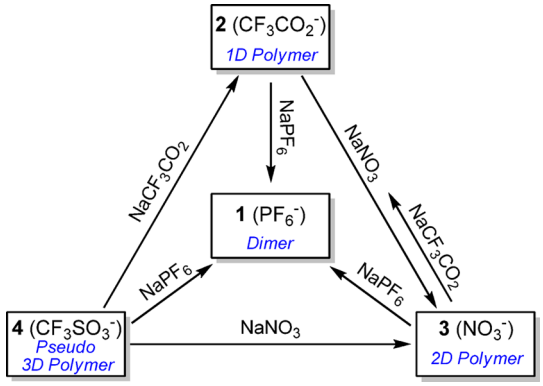

knowledge, the present anion-exchange systems are the first examples of bifunctional macrocycle-based coordination polymers to show dimensional changes resulting from anion exchange in the crystalline state.

In order to investigate the mechanistic process of the anion exchange, single crystals of **2** before and after immersing to 3 M $NaNO_3$ aqueous solution were used for atomic force microscope (AFM). Apparently, the sample does not change size or shape but loses transparency and single crystallinity during anion exchange. The AFM images and profiles in Figure 10 reveal that the crystal surface undergoes significant transformation, suggesting a restructuring of the crystal surface. Within 10 min, for example, the relatively homogeneous and flat crystal surface of the sample (Figure 10a) becomes rough, showing holes and clefts (Figure 10b). Soon a new crystal phase appears and continues to grow across the crystal surface. The entire process is compete about after 12 h, resulting in the final surface of the anion-exchanged sample more regularly

DOI: 10.1021/acs.inorgchem.5b00422
Inorg. Chem. 2015, 54, 5372–5383

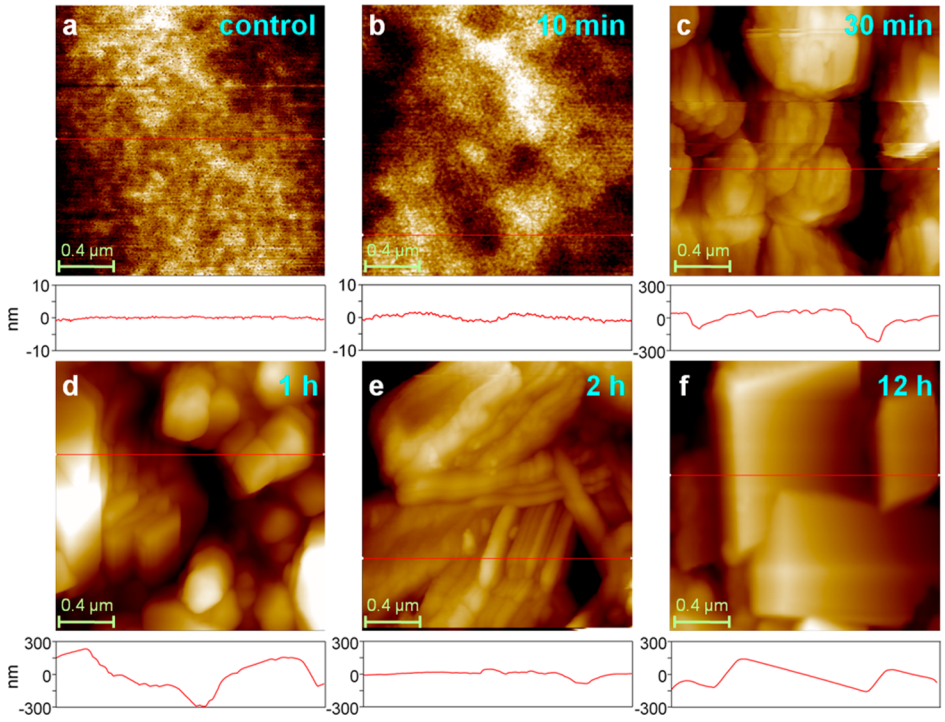

Figure 10. AFM images and profiles (bottom) of the surface of a crystal of **2** after immersing in 3 M $NaNO_3$ aqueous solution: (a) before anion-exchange, (b) 10 min, (c) 30 min, (d) 1 h, (e) 2 h, and (f) 12 h. Image size is 2 × 2 μm in all cases.

Scheme 5. Postulated Structural Conversion Process Accompanying the Dimensional Change from 1D (2) to 2D (3) by Anion Exchange in the Crystalline State

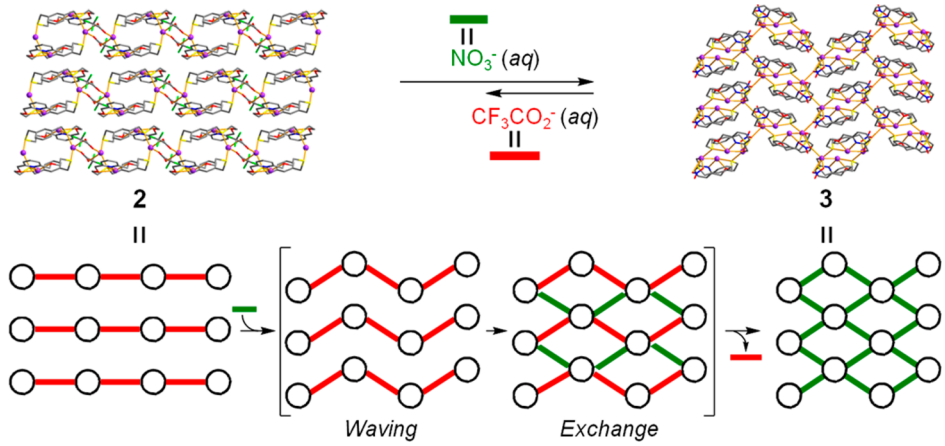

ordered and consists of microcrystallites. These observations are typical for solvent-mediated transformation,[26] which forms a new crystalline phase on the surface.

Although the detailed mechanism of the above structural transformations from **2** ($CF_3CO_2^-$, 1D) to **3** (NO_3^-, 2D) is not clear cut, we postulate the operation of a stepwise mechanistic process on the basis of the AFM images, PXRD patterns, IR spectra, and crystal packing structures as depicted in Scheme 5. Considering the packing structure of **2** and the network pattern of **3** shown in the top of Scheme 5, on immersing in an aqueous solution of NO_3^-, the crystalline sample of **2** with a parallel packing of 1D chains could be rearranged to give a waved intermediate with a herringbone packing pattern followed by initiation of anion exchange. Then the intermediate is considered to be converted to the final nitrate-containing 2D structure by replacing $CF_3CO_2^-$ with NO_3^- through the solvent-mediated dissolution (bond-breaking) and recrystallization (bond-making) process.[26]

CONCLUSION

In this work, a rationally designed NO_2S_2-macrocycle **L** that was expected to induce the formation of endo/exocoordinated network products was synthesized and this goal was realized. Indeed, the use of silver(I) allowed the formation of products with different metal coordination modes that included endo- and/or exocyclic binding. Furthermore, depending on the silver salt employed for complexation, a discrete cyclic dimer (**1**) and three polymeric products with 1D (**2**), 2D (**3**), and pseudo 3D (**4**) structures were isolated. The formation of the dinuclear sandwich-type cyclic dimer **1** appears to be mainly influenced by the presence of the large S···S distance in **L** and the noncoordinating behavior of the PF_6^-.

DOI: 10.1021/acs.inorgchem.5b00422
Inorg. Chem. 2015, 54, 5372−5383

In both **2** (1D with trifluoroacetate anion) and **3** (2D with nitrate anion), the tetranuclear bis(macrocycle) complex units are linked by anion coordination in a bridging bidentate manner to give infinite structures. However, $CF_3CO_2^-$ in **2** induces the formation of a 1D polymeric chain, while NO_3^- in **3** results in the formation of a 2D network product. In **2**, two bridging $CF_3CO_2^-$ ions form an octagonal metallacycle with two exocyclic Ag atoms. Thus, it is the networking via two $CF_3CO_2^-$ ions that results in the propagation of the single metallacyclic units in one direction to generate the 1D polymeric chain. This behavior appears mainly due to the steric hindrance of the large trifluoromethyl group and the preferred tendency to form a cyclic structure via H bonding or metal coordination. Unlike **2**, two nitrate ions in **3** propagate in two directions resulting in the formation of the 2D network. The smaller size and variable coordination modes of the nitrate ion are apparently advantageous in aiding the generation of this higher dimensional product.

The same reaction with silver(I) trifluoromethanesulfonate induced the formation of the pseudo 3D product **4** in which the endocyclic Ag atoms link macrocycles to generate 1D chains which are further cross-linked by the exocyclic Ag atoms to form a brick-wall-type 2D polymeric structure. The interligand $\pi-\pi$ stacking between the layers yields a pseudo 3D polymeric structure. In this case, the anion acts as a terminal monodentate ligand.

It is interesting that the respective products obtained share some common structural features. First, one silver(I) occupies the center of the macrocyclic cavity undoubtedly reflecting the presence of the pyridine subunit. Second, except for **1** where **L** binds to one silver(I) via NO_2S donors and another silver(I) through a Ag−S bond, the exocyclic silver(I) links the endocyclic complex units. Third, depending on the anion coordination mode, different topological products were prepared.

For the anion-exchange experiments in the crystalline state, all products displayed anion-exchange abilities that followed the following order: PF_6^- (**1**) > NO_3^- (**3**) > CF_3CO_2 (**2**) > $CF_3SO_3^-$ (**4**). The preference for PF_6^- and the lowest affinity for $CF_3SO_3^-$ indicate Hofmeister behavior. On the basis of the structural transformation from **2** ($CF_3CO_2^-$, 1D) to **3** (NO_3^-, 2D), the stepwise solvent-mediated mechanistic process shown previously was proposed.

From these results, it is concluded that the use of the ditopic macrocycle **L** enabled us to prepare new types of endo/exocyclic network complexes with their coordination modes and dimensions also under anion control both in the synthetic stage and also via anion exchange in the crystalline state. Further investigations of these and related novel supramolecular complexes displaying different coordination modes along with their applications are in progress.

EXPERIMENTAL SECTION

General. All chemicals and solvents used in the syntheses were of reagent grade and used without further purification. NMR spectra were recorded on a Bruker 300 spectrometer (300 MHz). The FT-IR spectra were measured with a Nicolet *i*S10 spectrometer. The ESI-mass spectra were obtained on a Thermo Scientific LCQ Fleet spectrometer. The elemental analysis was carried out on a Thermo Scientific Flash 2000 Series elemental analyzer. Thermogravimetric analyses were recorded in a TA Instruments TGA-Q50 thermogravimetric analyzer. Samples were heated at a constant rate of 5 °C min^{-1} from room temperature to 900 °C in a continuous-flow nitrogen atmosphere. The powder X-ray diffraction (PXRD) experiments were performed in a transmission mode with a Bruker GADDS diffractometer equipped with graphite-monochromated Cu Kα radiation (λ = 1.54073 Å). Atomic force microscope (AFM) imaging was performed in a noncontact mode under the following conditions: scan rate of 0.6 Hz; PPP-NCHR 10 M cantilever (Park systems).

Synthesis and Characterization of L. The precursor diol **5**[15a] (2.00 g, 7.74 mmol) was dissolved in anhydrous THF (30 mL) and added dropwise to a stirred suspension of NaH (0.47 g, 19.6 mmol) in anhydrous THF (50 mL) under nitrogen. After addition of the diol at room temperature, the mixture was refluxed for 1 h and then cooled to 0 °C. 2,6-Bis(tosyloxymethyl)pyridine **6**[15b] (3.47 g, 7.75 mmol) was dissolved in anhydrous THF (40 mL) and added slowly dropwise to the reaction mixture. The reaction mixture was rapidly stirred for 48 h at room temperature and then evaporated. The residue was partitioned between water and dichloromethane. The aqueous phase was separated and extracted with two further portions of dichloromethane. The combined organic phases were dried with anhydrous sodium sulfate and then evaporated to dryness. The flash column chromatography (SiO_2; dichloromethane−ethyl acetate 8:2) afforded the product as a white solid in 30% yield. Mp: 102−104 °C. ^{1}H NMR (300 MHz, $CDCl_3$): δ 7.70 (*s*, 1H, Ar), 7.30−7.19 (*m*, 5 H, Ar), 7.11 (*s*, 1 H, Ar), 4.61 (*s*, 4 H, ArCH_2O), 3.74 (*s*, 4 H, ArCH_2OS), 3.71 (*t*, 4 H, SCH_2CH$_2$O), 2.56 (*t*, 4 H, SCH$_2$CH_2O). ^{13}C NMR (75 MHz, $CDCl_3$): 157.59, 138.45, 137.23, 130.26, 129.16, 127.41, 121.73, 73.74, 70.97, 36.06, 29.66. IR (KBr pellet): 3040, 2957, 2919, 2899, 2846, 1591, 1577, 1454, 1418, 1360, 1343, 1152, 1110, 1086, 1040, 1022, 801, 765, 727, 708 cm^{-1}. Anal. Calcd for $[C_{19}H_{23}N_1O_2S_2]$: C, 63.13; H, 6.41; N, 3.87; S, 17.74. Found: C, 62.86; H, 6.51; N, 3.88; S, 17.49. Mass spectrum: m/z = 362.16 $[C_{19}H_{24}N_1S_4]^+$.

Preparation of $[Ag_2L_2](PF_6)_2$ (1). In a glass tube, silver(I) hexafluorophosphate (11.1 mg, 0.044 mmol) in methanol (2 mL) was layered onto a solution of **L** (10.5 mg, 0.029 mmol) in dichloromethane (2 mL). The X-ray quality colorless crystalline product **1** was obtained. Yield: 60%. Mp: 234−236 °C (decomp.). IR (KBr pellet): 3023, 2907, 2869, 1603, 1579, 1449, 1417, 1368, 1292, 1167, 1111, 1086, 1046, 841, 761, 706 cm^{-1}. Anal. Calcd for $[C_{38}H_{46}Ag_2P_2F_{12}N_2O_4S_4]$: C, 37.15; H, 3.77; N, 2.28; S, 10.44. Found: C, 37.05; H, 3.94; N, 2.28; S, 10.58.

Preparation of $[Ag_4L_2(CF_3CO_2)_4]_n$ (2). Silver(I) trifluoroacetate (9.5 mg, 0.043 mmol) in methanol (2 mL) was added to a solution of **L** (10.2 mg, 0.028 mmol) in dichloromethane (2 mL). Slow evaporation of the solution afforded a colorless crystalline product **2** suitable for X-ray analysis. Yield: 70%. Mp: 220−222 °C (decomp.). IR (KBr pellet): 3039, 2957, 2921, 2849, 1685, 1639, 1593, 1578, 1459, 1424, 1362, 1208, 1129, 1087, 1042, 1023, 838, 802, 723, 710 cm^{-1}. Anal. Calcd for $[C_{46}H_{46}Ag_4F_{12}N_2O_{12}S_4]$: C, 34.39; H, 2.89; N, 1.74; S, 7.98. Found: C, 34.52; H, 2.83; N, 1.74; S, 8.08.

Preparation of $[Ag_4L_2(NO_3)_4]_n$ (3). Silver(I) nitrate (6.5 mg, 0.042 mmol) in methanol (2 mL) was added to a solution of **L** (10.2 mg, 0.028 mmol) in dichloromethane (2 mL). Slow evaporation of the solution afforded a colorless crystalline product **3** suitable for X-ray analysis. Yield: 75%. Mp: 206−208 °C. IR (KBr pellet): 3022, 2922, 2860, 1599, 1578, 1480, 1440, 1383, 1301, 1133, 1106, 1088, 1033, 1004, 933, 813, 791, 710 cm^{-1}. Anal. Calcd for $[C_{38}H_{46}Ag_4N_6O_{16}S_4]$: C, 32.54; H, 3.31; N, 5.99; S, 9.14. Found: C, 32.37; H, 3.31; N, 5.90; S, 8.82.

Preparation of $\{[Ag_3L_2(CF_3SO_3)_2]CF_3SO_3\}_n$ (4). Silver(I) trifluoromethanesulfonate (8.5 mg, 0.033 mmol) in methanol (2 mL) was added to a solution of **L** (10.2 mg, 0.028 mmol) in dichloromethane (2 mL). Slow evaporation of the solution afforded a colorless crystalline product **4** suitable for X-ray analysis. Yield: 65%. Mp: 202−204 °C. IR (KBr pellet): 3073, 2999, 2920, 2872, 1604, 1578, 1471, 1445, 1366, 1279, 1260, 1225, 1165, 1110, 1085, 1050, 1026, 997, 901, 809, 797, 781, 757, 707 cm^{-1}. Anal. Calcd for $[C_{41}H_{46}Ag_3F_9N_2O_{13}S_7]$: C, 32.97; H, 3.10; N, 1.88. Found: C, 33.26; H, 3.11; N, 1.93.

Anion Exchange. The anion-exchange experiments were performed with complexes **1**−**4** (5 mg) by immersing in a 3 M aqueous solution (2 mL) of each corresponding sodium salt and leaving undisturbed at ambient temperature. Each solid sample was periodically collected by filtration, washed several times with distilled

DOI: 10.1021/acs.inorgchem.5b00422
Inorg. Chem. 2015, 54, 5372−5383

water, and then dried in air. The crystalline samples collected from the anion-exchange experiments were unacceptable for single-crystal X-ray diffraction analysis. Thus, the structural conversion associated with anion exchange was monitored by the PXRD patterns and their IR spectra.

X-ray Crystallographic Analysis. All data were collected on a Bruker SMART APEX II ULTRA diffractometer equipped with graphite-monochromated Mo Kα radiation (λ = 0.71073 Å) generated by a rotating anode. The cell parameters for the compounds were obtained from a least-squares refinement of the spot (from 36 collected frames). Data collection, data reduction, and semiempirical absorption correction were carried out using the software package of APEX2.[27] All of the calculations for the structure determination were carried out using the SHELXTL package.[28] In all cases, all nonhydrogen atoms were refined anisotropically and all hydrogen atoms were placed in idealized positions and refined isotropically in a riding manner along with the their respective parent atoms. Relevant crystal data collection and refinement data for the crystal structures of **1**−**4** are summarized in Table 1. In **3**, O3 and O5 atoms are disordered into two positions (64:36 and 50:50, respectively). In **4**, the noncoordinated $CF_3SO_3^-$ is disordered about the special position, and its F5 atom is disordered over two positions (50:50). The "ISOR" command has been used in the refinement of **4** (O6).

■ ASSOCIATED CONTENT

Ⓢ Supporting Information

NMR spectra, additional crystal structures, PXRD patterns, IR spectra, and X-ray crystallographic files (CIFs). CCDC-1047895 (**L**), -1047896 (**1**), -1047897 (**2**), -1047898 (**3**), and -1047899 (**4**) contain the supplementary crystallographic data for this paper. These data can be obtained free of charge from The Cambridge Crystallographic Data Center via www.ccdc.cam.ac.uk/data_request/cif. The Supporting Information is available free of charge on the ACS Publications website at DOI: 10.1021/acs.inorgchem.5b00422.

■ AUTHOR INFORMATION

Corresponding Authors

*E-mail: habata@chem.sci.toho-u.ac.jp.

*E-mail: sslee@gnu.ac.kr.

Notes

The authors declare no competing financial interest.

■ ACKNOWLEDGMENTS

This work was supported from NRF (2012R1A4A1027750 and 2013R1A2A2A01067771), S. Korea, and the Supported Program for Strategic Research Foundation at Private Universities (2012−2016) from the Ministry of Education, Culture, Sports, Science and Technology of Japan. E.L. acknowledges the support by NRF-2013-Fostering Core Leaders of the Future Basic Science Program.

■ REFERENCES

(1) (a) Batten, S. R.; Robson, R. *Angew. Chem., Int. Ed.* **1998**, *37*, 1460. (b) Eddaoudi, M.; Moler, D. B.; Li, H.; Chen, B.; Reineke, T. M.; O'Keeffe, M.; Yaghi, O. M. *Acc. Chem. Res.* **2001**, *34*, 319. (c) Kitagawa, S.; Matsuda, R. *Coord. Chem. Rev.* **2007**, *251*, 2490. (d) Kawano, M.; Fujita, M. *Coord. Chem. Rev.* **2007**, *251*, 2592. (e) Northrop, B. H.; Zheng, Y.-R.; Chi, K.-W.; Stang, P. J. *Acc. Chem. Res.* **2009**, *42*, 1554. (f) Murray, L. J.; Dincă, M.; Long, J. R. *Chem. Soc. Rev.* **2009**, *38*, 1294. (g) Lindoy, L. F.; Park, K.-M.; Lee, S. S. *Chem. Soc. Rev.* **2013**, *42*, 1713.

(2) (a) Izatt, R. M.; Pawlak, K.; Bradshaw, J. S. *Chem. Rev.* **1991**, *91*, 1721. (b) Lindoy, L. F. *Coord. Chem. Rev.* **1998**, *174*, 327. (c) Izatt, R. M.; Pawlak, K.; Bradshaw, J. S. *Chem. Rev.* **1995**, *95*, 2529.

(3) (a) Choi, H.-S.; Suh, M. P. *Angew. Chem., Int. Ed.* **2009**, *48*, 6865. (b) Janzen, D. E.; Botros, M. E.; VanDerveer, D. G.; Grant, G. J. *Dalton Trans.* **2007**, 5316. (c) Lee, S. J.; Hupp, J. T. *Coord. Chem. Rev.* **2006**, *250*, 1710.

(4) (a) Muthu, S.; Yip, J. H. K.; Vittal, J. J. *J. Chem. Soc., Dalton Trans.* **2002**, 4561. (b) Custelcean, R.; Moyer, B. A. *Eur. J. Inorg. Chem.* **2007**, 1321. (c) Zhao, W.; Fan, J.; Okamura, T.; Sun, W.-Y.; Ueyama, N. *New J. Chem.* **2004**, *28*, 1142. (d) Du, M.; Guo, Y.-M.; Chen, S.-T.; Bu, X.-H. *Inorg. Chem.* **2004**, *43*, 1287. (e) Sarkar, M.; Biradha, K. *Cryst. Growth Des.* **2007**, *7*, 1318. (f) Tzeng, B.-C.; Chiu, T.-H.; Chen, B.-S.; Lee, G.-H. *Chem.—Eur. J.* **2008**, *14*, 5237. (g) Liu, J.-Y.; Wang, Q.; Zhang, L.-J.; Yuan, B.; Xu, Y.-Y.; Zhang, X.; Zhao, C.-Y.; Wang, D.; Yuan, Y.; Wang, Y.; Ding, B.; Zhao, X.-J.; Yue, M. M. *Inorg. Chem.* **2014**, *53*, 5972. (h) Hashemi, L.; Morsali, A.; Büyükgüngor, O. *New J. Chem.* **2014**, *38*, 3187. (i) Halper, S. R.; Do, L.; Stork, J. R.; Cohen, S. M. *J. Am. Chem. Soc.* **2006**, *128*, 15255.

(5) (a) Park, S.; Lee, S. Y.; Park, K.-M.; Lee, S. S. *Acc. Chem. Res.* **2012**, *45*, 391. (b) Lee, E.; Lee, S. Y.; Lindoy, L. F.; Lee, S. S. *Coord. Chem. Rev.* **2013**, *257*, 3125.

(6) (a) Wolf, R. E., Jr.; Hartman, J. R.; Storey, J. M. E.; Foxman, B. M.; Cooper, S. R. *J. Am. Chem. Soc.* **1987**, *109*, 4328. (b) Blake, A. G.; Schröder, M. *Adv. Inorg. Chem.* **1990**, *35*, 1. (c) Hill, S. E.; Feller, D. *J. Phys. Chem. A* **2000**, *104*, 652.

(7) (a) Lee, S. Y.; Lee, S. S. *Inorg. Chem.* **2010**, *12*, 3471. (b) Kim, H. J.; Lindoy, L. F.; Lee, S. S. *Cryst. Growth Des.* **2010**, *10*, 3850. (c) Kim, H. J.; Park, I.-H.; Lee, J.-E.; Park, K.-M.; Lee, S. S. *Cryst. Growth Des.* **2014**, *14*, 6269.

(8) (a) Kim, H. J.; Lee, S. S. *Inorg. Chem.* **2008**, *47*, 10807. (b) Kim, H. J.; Sultana, K. F.; Lee, J. Y.; Lee, S. S. *CrystEngComm* **2010**, *12*, 1494. (c) Lee, H.-H.; Park, I.-H.; Lee, S. S. *Inorg. Chem.* **2014**, *53*, 4763.

(9) (a) Yoon, I.; Seo, J.; Lee, J.-E.; Park, K.-M.; Kim, J. S.; Lah, M. S.; Lee, S. S. *Inorg. Chem.* **2006**, *45*, 3487. (b) Jin, Y.; Kim, H. J.; Lee, J. Y.; Lee, S. Y.; Shim, W. J.; Hong, S. H.; Lee, S. S. *Inorg. Chem.* **2010**, *49*, 10241. (c) Lee, E.; Lee, S. S. *Inorg. Chem.* **2011**, *50*, 5803. (d) Kim, J.-Y.; Park, I.-H.; Lee, J. Y.; Lee, J.-H.; Park, K.-M.; Lee, S. S. *Inorg. Chem.* **2013**, *52*, 10176. (e) Ryu, H.; Park, K.-M.; Ikeda, M.; Habata, Y.; Lee, S. S. *Inorg. Chem.* **2014**, *53*, 4029.

(10) Lee, E.; Lee, S. S. *CrystEngComm* **2013**, *15*, 1814.

(11) (a) Lee, S. J.; Jung, J. H.; Seo, J.; Yoon, I.; Park, K.-M.; Lindoy, L. F.; Lee, S. S. *Org. Lett.* **2006**, *8*, 1641. (b) Lee, H.; Lee, S. S. *Org. Lett.* **2009**, *11*, 1393.

(12) Lee, S. J.; Lee, J.-E.; Seo, J.; Lee, S. S.; Jung, J. H. *Adv. Funct. Mater.* **2007**, *17*, 3441.

(13) (a) Kang, E.-J.; Lee, S. Y.; Lee, H.; Lee, S. S. *Inorg. Chem.* **2010**, *49*, 7510. (b) Seo, J.; Song, M. R.; Lee, J.-E.; Lee, S. Y.; Yoon, I.; Park, K.-M.; Kim, J.; Jung, J. H.; Park, S. B.; Lee, S. S. *Inorg. Chem.* **2006**, *45*, 952. (c) Kumar, S.; Hundal, M. S.; Hundal, G.; Singh, P.; Bhalla, V.; Singh, H. *J. Chem. Soc., Perkin Trans. 2* **1998**, 925.

(14) (a) Lee, S. Y.; Park, S.; Kim, H. J.; Jung, J. H.; Lee, S. S. *Inorg. Chem.* **2008**, *47*, 1913. (b) Lee, S. Y.; Seo, J.; Yoon, I.; Kim, C.-S.; Choi, K. S.; Kim, J. S.; Lee, S. S. *Eur. J. Inorg. Chem.* **2006**, 3525.

(15) (a) de Groot, B.; Loeb, S. J.; Shimizu, G. K. H. *Inorg. Chem.* **1994**, *33*, 2663. (b) Constable, E. C.; King, A. C.; Raithby, P. R. *Polyhedron* **1998**, *17*, 4275.

(16) Addison, A. W.; Rao, T. N.; Reedijk, J.; Van Rijin, J.; Verschoor, G. C. *J. Chem. Soc., Dalton Trans.* **1984**, 1349.

(17) (a) *MOGUL*; Cambridge Crystallographic Database: Cambridge, U.K., 2006. (b) Lee, S. Y.; Park, S.; Seo, J.; Lee, S. S. *Inorg. Chem. Commun.* **2007**, *10*, 1102.

(18) Jung, O.-S.; Kim, Y. J.; Lee, Y.-A.; Park, K.-M.; Lee, S. S. *Inorg. Chem.* **2003**, *42*, 844.

(19) (a) Brammer, L.; Burgard, M. D.; Rodger, C. S.; Swearingen, J. K.; Rath, N. R. *Chem. Commun.* **2001**, 2468. (b) Lu, X. L.; Leong, W. K.; Goh, L. Y.; Hor, A. T. S. *Eur. J. Inorg. Chem.* **2004**, 2504.

(20) Dance, I.; Scudder, M. *J. Chem. Soc., Chem. Commun.* **1995**, 1039−1040.

(21) (a) Kim, H. J.; Song, M. R.; Lee, S. Y.; Lee, J. Y.; Lee, S. S. *Eur. J. Inorg. Chem.* **2008**, 3532. (b) Park, S.; Lee, S.-G.; Jung, J. H.; Ikeda, M.;

DOI: 10.1021/acs.inorgchem.5b00422
Inorg. Chem. 2015, 54, 5372−5383

Habata, Y.; Lee, S. S. *CrystEngComm* **2012**, *14*, 6515. (c) Liang, G.; Liu, Y.; Zhang, X.; Yi, Z. *CrystEngComm* **2014**, *16*, 9896. (d) Feng, Y.; Wang, D.-B.; Wan, B.; Li, X.-H.; Shi, Q. *Inorg. Chim. Acta* **2014**, *413*, 187.

(22) (a) Haj, M. A.; Aakeröy, C. B.; Desper, J. *New J. Chem.* **2013**, *37*, 204. (b) Pogozhev, D.; Baudron, S. A.; Hosseini, M. W. *Dalton Trans.* **2011**, *40*, 437. (c) Pocic, D.; Planeix, J.-M.; Kyritsakas, N.; Jouaiti, A.; Hosseini, M. W. *CrystEngComm* **2005**, *7*, 624. (d) Khlobystov, A. N.; Blake, A. J.; Champness, N. R.; Lemenovskii, D. A.; Majouga, A. G.; Zyk, N. V.; Schröder, M. *Coord. Chem. Rev.* **2001**, *222*, 155.

(23) (a) Archer, R. D.; Dardiman, C. J.; Lee, A. Y. In *Photochemistry and Photophysics of Coordination Compounds*; Yersin, H., Vogler, A., Eds.; Spriger-Verlag: Berlin, 1987; p 285. (b) Valeur, B. *Molecular Fluorescence: Principles and Applications*; Wiley-VCH: Weinheim, Germany, 2002.

(24) Hofmeister, F. *Arch. Exp. Pathol. Pharmakol.* **1888**, *24*, 247.

(25) (a) Min, K. S.; Suh, M. P. *J. Am. Chem. Soc.* **2000**, *122*, 6834. (b) Jung, O.-S.; Kim, Y. J.; Lee, Y.-A.; Chae, H. K.; Jang, H. G.; Hong, J. *Inorg. Chem.* **2001**, *40*, 2105. (c) Noro, S.-i.; Kitaura, R.; Kondo, M.; Kitagawa, S.; Ishii, T.; Matsuzaka, H.; Yamashita, M. *J. Am. Chem. Soc.* **2002**, *124*, 2568. (d) Wu, J.-Y.; Liu, Y.-C.; Chao, T.-C. *Inorg. Chem.* **2014**, *53*, 5581.

(26) (a) Wei, W.; Yu, H.; Jiang, F.; Liu, B.; Ma, J.; Hong, M. *CrystEngComm* **2012**, *14*, 1693. (b) Yang, H.; Li, L.; Wu, J.; Hou, H.; Xiao, B.; Fan, Y. *Chem.—Eur. J.* **2009**, *15*, 4049. (c) Khlobystov, A. N.; Champness, N. R.; Roberts, C. J.; Tendler, S. J.B.; Thompson, C.; Schröder, M. *CrystEngComm* **2002**, *4*, 426. (d) Thompson, C.; Champness, N. R.; Khlobystov, A. N.; Roberts, C. J.; Schröder, M.; Tendler, S. J. B.; Wilkinson, M. J. *J. Microsc.* **2004**, *214*, 261. (e) Rodriguez-hornedo, N.; Murphy, D. *J. Pharm. Sci.* **1999**, *88*, 651. (f) Booth, J.; Compton, R. G.; Atherton, J. H. *J. Phys. Chem. B* **1998**, *102*, 3980. (g) Booth, J.; Hong, Q.; Compton, R. G.; Prout, K.; Payne, R. M. *J. Colloid Interface Sci.* **1997**, *192*, 207. (h) Pina, C. M.; Fernandez-Diaz, L.; Prieto, M.; Putnis, A. *Geochim. Cosmochim. Acta* **2000**, *64*, 215. (i) Malkin, A. J.; Kuznetsov, Yu. G.; McPherson, A. *J. Cryst. Growth* **1999**, *196*, 471.

(27) *APEX 2 Bruker, SAINT (ver. 6.22): Area Detector Control and Integration Software*; Bruker AXS Inc.: Madison, WI, 2000.

(28) *SHELXTL (ver. 6.10): Program for Solution and Refinement of Crystal Structures*; Bruker AXS Inc.: Madison, WI, 2000.

DOI: 10.1021/acs.inorgchem.5b00422
Inorg. Chem. 2015, 54, 5372−5383